PCCP

ROYAL SOCIETY OF CHEMISTRY

PAPER

View Article Online
View Journal | View Issue

Cite this: *Phys. Chem. Chem. Phys.*, 2024, **26**, 24461

The effect of Ficoll 70 on thermally-induced and chemically-induced conformational transitions of an RTX protein is quantitatively accounted for by a unified excluded volume model†

Alexandre Chenal *[a] and Allen P. Minton *[b]

Received 29th May 2024,
Accepted 27th August 2024

DOI: 10.1039/d4cp02213k

rsc.li/pccp

A unified excluded volume model based upon the effective hard particle approximation is developed and used to quantitatively model previously published experimental measurements of the effect of adding high concentrations of an "inert" polymer, Ficoll 70, on conformational transitions of the toxin protein RCL that are induced by addition of calcium at constant temperature or by increasing temperature in the absence and presence of high calcium concentrations. The best-fit of this model, which accounts quantitatively for all of the published data to within experimental precision, yields an estimate of the volume of solution excluded to Ficoll by each of four identified conformational states of RCL: H – the most compact conformation adopted in the limits of high calcium concentration and low temperature, H* – the conformation adopted in the limits of high calcium concentration and high temperature, A – the conformation adopted in the limits of low (or no) calcium at low temperature, and A* – the conformation adopted in the limits of low calcium and high temperature. Ficoll exclusion volumes increase in the order H < H* < A < A*. These results are discussed in the context of the physiological functions of the RTX proteins, which are involved in the secretion process and the calcium-induced folding of bacterial virulence factors.

I. Introduction

In 2013, Sotomayor-Peréz *et al.* published a study on the effect of high concentrations of an "inert" polymer, Ficoll 70, upon the conformational changes of a repeat-in-toxin (RTX[1]) protein, RCL.[2] RCL is a polypeptide corresponding to the Block V of the adenylate cyclase (CyaA) toxin and its C-terminal flanking region (residues 1530 to 1680 of CyaA). The CyaA toxin is produced by *Bordetella pertussis*, the causative agent of the whooping cough.[3–6] The primary sequence of RCL is described in supporting files of Sotomayor Perez *et al.*[2] The present work is an extension of that study, and we shall refer to it henceforth as SP. It has been shown that RCL constitutes an autonomous RTX calcium-binding protein[1,7] required for folding, and both cytotoxic and hemolytic activities of the full-length CyaA toxin.[8–12] In the absence of calcium, apo-RCL exhibits the hallmarks of intrinsically disordered proteins.[7,13,14] Its unfolded and flexible ensemble of conformations in the apo-state result from internal electrostatic repulsion between negatively charged residues.[15] The apo-state of RTX proteins is appropriately sized for its bacterial uptake and secretion through the narrow channel of their dedicated secretion systems (internal diameter of 2 nm) and acquires its folded and stable holo-conformation upon secretion in the calcium-rich lung environment.[16,17] The calcium-induced folding of RTX proteins is finely regulated by the calcium gradient across the bacterial cell wall.[18] Calcium binding causes a strong reduction of the mean net charge and local structuring of Ca binding sites, thereby triggering the compaction, folding and stabilization of holo-RCL.[7,15]

The study of SP was and remains unique among many studies of the effect of high concentrations of a chemically "inert" species upon the conformation of a dilute or trace species of protein (reviewed by Speer *et al.*[19]) for the following reason. Experiments were carried out by SP on solutions of

[a] *Institut Pasteur, Université de Paris Cité, CNRS UMR3528, Biochemistry of Macromolecular Interactions Unit, F75015 Paris, France. E-mail: alexandre.chenal@pasteur.fr*

[b] *Laboratory of Biochemistry and Genetics, National Institute of Diabetes and Digestive and Kidney Diseases, National Institutes of Health, Bethesda, Maryland, USA. E-mail: allenm@nih.gov, allenpminton@gmail.com*

† Electronic supplementary information (ESI) available: Relation between abundance of a conformational state and an experimentally measurable signal. Table S1 best fit parameter values from two-state modeling of conformational change as a function of calcium concentration at 25 °C. Table S2 best fit parameter values obtained from two-state modeling of conformational change as a function of temperature for the thermally induced unfolding of H at high Ca concentration and thermally induced unfolding of A in the absence of Ca. See DOI: **https://doi.org/10.1039/d4cp02213k**

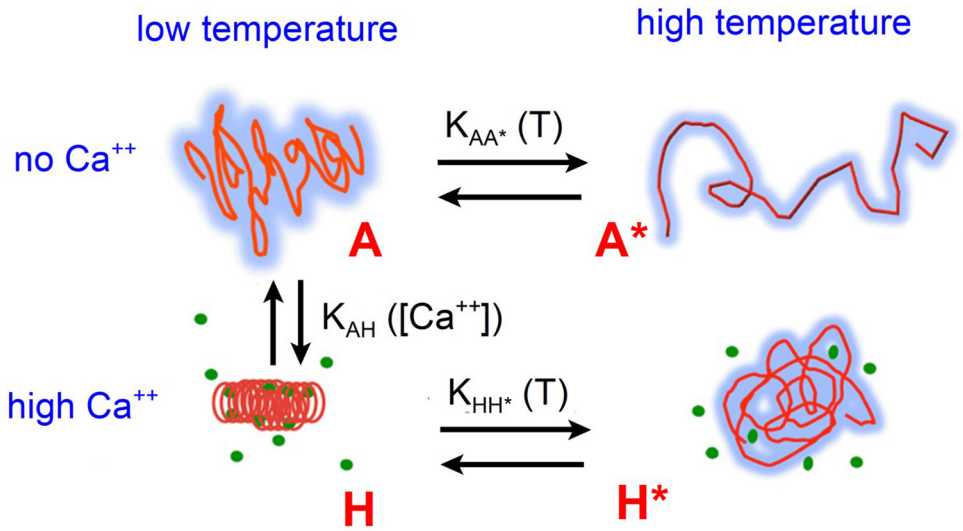

Fig. 1 Schematic illustration of the four conformational states of RCL, as proposed by SP. Figure adapted from SP.

identical composition to characterize crowding effects upon thermal unfolding in the absence and presence of high concentrations of calcium (Ca), as well as the effect of Ficoll concentration on the binding of Ca upon protein folding at constant temperature. Thus, the effect of crowding upon both thermally-induced unfolding and chemically-induced unfolding (*via* loss of a structure-stabilizing binding partner, *i.e.*, calcium) of the same protein under comparable conditions was quantitatively characterized.[2]

Analysis of the results of these and other experiments led SP to propose the existence of four distinguishable conformational states of RCL, schematically illustrated in Fig. 1: (1) fully folded holo-RCL in the low temperature limit in the presence of saturating concentrations of Ca, which we shall refer to as holo-state (H), (2) partially unfolded apo-RCL in the low temperature limit in the absence of Ca, referred to as apo-state (A), (3) partially unfolded holo-RCL in the high temperature limit in the presence of Ca, referred to as high-temp holo-state (H*) and (4) fully unfolded apo-RCL at the high temperature limit in the absence of Ca, referred to as high-temp apo-state (A*).

SP provided experimental evidence that conformational transitions between H and H*, and between A and A*, may be characterized as two-state transitions. In the present work, we shall demonstrate that even though RCL contains multiple binding sites for Ca, the conformational transition between H and A may also be described to within experimental precision as two-state.

In Section II we summarize a simple excluded volume model for the effect of macromolecular crowding upon a generic two-state conformational transition. In Section III a quantitative model for the simultaneous effects of Ca binding and Ficoll 70 upon the conformational changes of RCL at constant (low) temperature is presented and the relevant data of SP analyzed in the context of this model. In Section IV the data of SP on the thermally-induced conformational transitions of H and A in the presence of different concentrations of Ficoll 70 are then newly analyzed in the context of the two-state theory of thermal unfolding,[20] extended in accordance with the excluded volume model presented in Section II. In Section V the results of analyzing both thermally and chemically induced conformational transitions are incorporated into a unified picture of the relative interaction between Ficoll 70 and each conformational state. It will be shown that the data provided by SP permit us to characterize quantitatively the relative nonspecific interactions of each conformational state with Ficoll 70, and demonstrate that these interactions may be described to within experimental precision as independent of temperature, and hence primarily entropic in nature. The significance and potential biological relevance of the findings reported here is discussed in the concluding section.

II. First-order excluded volume model for the effect of molecular crowding on a two-state conformational transition

The effect of thermodynamic nonideality upon the equilibrium between two conformations of a protein or other macromolecule in solution (generically labeled here as conformations 1 and 2) is described by

$$K_{12} \equiv \frac{c_2}{c_1} = K_{12}^0 \frac{\gamma_1}{\gamma_2} \tag{1}$$

where c_i and γ_i denote the molar concentration and thermodynamic activity coefficient of species i respectively, and K_{12}^0 denotes the equilibrium constant in the ideal limit, *i.e.*, when all γ_i approach unity.[21] Eqn (1) is equivalent to

$$\ln K_{12} = \ln K_{12}^0 + \ln \gamma_1 - \ln \gamma_2. \tag{2}$$

We consider the case in which a trace amount of the protein under consideration ('tracer') is dissolved in a solution containing a significantly higher concentration of an inert macromolecule

('crowder') that interacts with the trace protein. In this case the activity coefficient of each conformational state of the trace protein is given to first order by

$$\ln \gamma_i = B_{i\mathrm{C}} c_{\mathrm{C}} \tag{3}$$

where c_{C} denotes the molar concentration of crowder, and $B_{i\mathrm{C}}$ denotes the two-body interaction coefficient, which is a function of the potential of mean force acting between state i and crowder.[22] According to the effective hard particle model,[23–25] $B_{i\mathrm{C}}$ may be expressed as a volume that is excluded by an effective hard particle representing a molecule of the ith conformation of tracer to the center of mass of a second effective hard particle representing a molecule of crowder (or the volume that is excluded to crowder to the ith conformation of tracer). This volume is referred to as the covolume of the ith tracer conformation and crowder,[26] denoted by $V_{i\mathrm{C}}$. Within the context of the effective hard particle model, eqn (3) is equivalent to

$$\ln \gamma_i = V_{i\mathrm{C}} c_{\mathrm{C}} \tag{4}$$

Combination of eqn (2) and (4) leads to

$$\ln K_{12} = \ln K_{12}^0 + \alpha_{12} c_{\mathrm{C}} \tag{5}$$

where $\alpha_{12} \equiv V_{1\mathrm{C}} - V_{2\mathrm{C}}$, and $\alpha_{21} = -\alpha_{12}$.

According to the excluded volume model, the effect of excluded volume (quantified by the parameter α_{12}) is orthogonal to and independent of changes in other experimental variables that would contribute to changes in the value of K_{12}^0, such as changes in temperature or binding of ligand to tracer. In addition, we note that when two different two-state conformational transitions have one conformation in common, such as $\{1\} \rightleftarrows \{2\}$ and $\{2\} \rightleftarrows \{3\}$, then it follows from eqn (3) and (4) that

$$\alpha_{13} = \alpha_{12} + \alpha_{23}. \tag{6}$$

We shall subsequently apply this model to the analysis of the results of experiments by SP that measure the effect of Ficoll 70 on the equilibria between holo and high-temp holo, between apo and high-temp apo, and between holo and apo at 25 °C. Far-UV circular dichroism (CD) spectra of holo-RCL as a function of temperature in the absence and in the presence of 200 g l^{-1} Ficoll 70 presented in SP (Fig. 3A and Fig. S3, see ref. 2) indicate that the conformational transitions between holo and high-temp holo in the absence presence and presence of Ficoll are two-state, and that Ficoll does not significantly affect the secondary structure of either holo or high temp holo. The results of CD and tryptophan fluorescence ratios presented in SP (Fig. S4–S6, see ref. 2) also indicate that the secondary and tertiary structures of RCL at low and high temperatures are very similar in the absence and presence of 200 g l^{-1} Ficoll, suggesting that Ficoll has little if any effect upon the secondary/tertiary structures of the conformational states of RCL either at low or high temperature, but has a significant effect upon the equilibrium between these states.

III. Dependence of RCL conformation upon the concentrations of Ca and Ficoll 70 at 25 °C

A. Excluded volume model

The two-state allosteric model presented below derives from that developed originally by Monod, Wyman and Changeux,[27] with generalization to allow for thermodynamic nonideality attributed to volume exclusion. We assume that RCL can exist in either the apo (A) or holo (H) state at 25 °C. We define the thermodynamic conformational equilibrium constant

$$L_0 = \frac{a_{\mathrm{H}_0}}{a_{\mathrm{A}_0}} = \frac{\gamma_{\mathrm{H}_0}[\mathrm{H}_0]}{\gamma_{\mathrm{A}_0}[\mathrm{A}_0]} \tag{7}$$

where a_{H_0}, γ_{H_0}, and $[\mathrm{H}_0]$ respectively denote the thermodynamic activity, the thermodynamic activity coefficient, and molar concentration of H in the absence of Ca, and a_{A_0}, γ_{A_0}, and $[\mathrm{A}_0]$ respectively denote the same three properties of A in the absence of Ca. We may then define the apparent equilibrium constant

$$L \equiv \frac{[\mathrm{H}_0]}{[\mathrm{A}_0]} = L_0 \frac{\gamma_{\mathrm{A}_0}}{\gamma_{\mathrm{H}_0}}. \tag{8}$$

We next assume that both A and H states contain n identical and independent binding sites for calcium, with equilibrium association constants for binding Ca to an individual site given by K_{A} and K_{H} respectively. Thus, the equilibrium concentration of the species of A binding i molecules of Ca may be written:

$$[\mathrm{A}_i] = [\mathrm{A}_0] \begin{bmatrix} n \\ i \end{bmatrix} (K_{\mathrm{A}} a_{\mathrm{Ca}})^i. \tag{9}$$

where a_{Ca} denotes the thermodynamic activity of Ca, and $\begin{bmatrix} n \\ i \end{bmatrix}$ denotes the number of microstates with i molecules of Ca bound to n sites, given by

$$\begin{bmatrix} n \\ i \end{bmatrix} = \frac{n!}{i!(n-i)!}. \tag{10}$$

The equilibrium concentration of the species of H binding i molecules of Ca may similarly be written

$$[\mathrm{H}_i] = [\mathrm{H}_0] \begin{bmatrix} n \\ i \end{bmatrix} (K_{\mathrm{H}} a_{\mathrm{Ca}})^i. \tag{11}$$

Let us define the ratio $z \equiv K_{\mathrm{H}}/K_{\mathrm{A}}$. Then equation [11] may be rewritten

$$[\mathrm{H}_i] = L z^i [\mathrm{A}_0] \begin{bmatrix} n \\ i \end{bmatrix} (K_{\mathrm{A}} a_{\mathrm{Ca}})^i = L z^i [A_i]. \tag{12}$$

The fractional saturation of binding sites by Ca at equilibrium may then be written as

$$y = \frac{\sum_{i=1}^{n} i([\mathrm{A}_i] + [\mathrm{H}_i])}{n \sum_{i=0}^{n} ([\mathrm{A}_i] + [\mathrm{H}_i])} = \frac{\sum_{i=1}^{n} i \begin{bmatrix} n \\ i \end{bmatrix} (1 + Lz^i)(K_{\mathrm{A}} a_{\mathrm{Ca}})^i}{n \sum_{i=0}^{n} \begin{bmatrix} n \\ i \end{bmatrix} (1 + Lz^i)(K_{\mathrm{A}} a_{\mathrm{Ca}})^i}. \tag{13}$$

The fraction of protein in the holo (H) state is given by

$$f_H = \frac{\sum_{i=0}^{n}[H_i]}{\sum_{i=0}^{n}([A_i]+[H_i])} = \frac{\sum_{i=0}^{n}\binom{n}{i}Lz^i(K_A a_{Ca})^i}{\sum_{i=0}^{n}\binom{n}{i}(1+Lz^i)(K_A a_{Ca})^i}. \quad (14)$$

Crowding by an inert molecule C (C for crowder) occupying volume fraction ϕ of the solution is assumed to affect the thermodynamic activity of the A and H states of protein and Ca. Assuming that Ca may occupy all of the volume available to solvent, the effect of volume occupancy by Ficoll upon Ca activity is relatively small:

$$a_{Ca} = [Ca]/(1-\phi) = [Ca]/(1-\bar{\nu}w_C). \quad ([15])$$

where $\bar{\nu}$ and w_C respectively denote the partial specific volume and w/v concentration of crowder. [The data provided by SP includes this correction, but in that publication, they referred to the activity of Ca as the "effective concentration".]

According to eqn (4), the activity coefficients of dilute A and H states are given by

$$\ln\gamma_X = V_{XC}\rho_C \quad (16)$$

where X denotes either A or H, and V_{XC} denotes the volume excluded by a molecule of conformational state X to a molecule of crowder, and ρ_C the number density of crowder molecules. It follows from eqn (4), (5) and (16) that

$$\ln L = \ln L_0 + (V_{AC} - V_{HC})\rho_C. \quad (17)$$

Since the covolumes, and hence $(V_{AC} - V_{HC})$ are assumed constant, and ρ_C is proportional to the w/v concentration of Ficoll, eqn (17) is equivalent to

$$\ln L = \ln L_0 + \alpha w_{Fic}. \quad (18)$$

Since ln L is dimensionless, the units of α are inverse concentration. It follows that if w_{Fic} in eqn (12) is expressed in units of g-Ficoll per cm^3, α denotes the difference between volume excluded to Ficoll by A and by H in cm^3 per gram of Ficoll.

B. Modeling the data

The model described above provides relations for the calculation of the value of f_H, the mass fraction of RCL in the holo (H) state as a function of the concentrations of Ca and Ficoll 70. Here we describe the procedure used to model experimental data obtained by SP, plotted in Fig. 2. These data consist of fractional change in the ratio of intrinsic tryptophan fluorescence at 360/320 nm (denoted subsequently by FIR for fluorescence intensity ratio) as a function of the thermodynamic activity or "effective concentration" of Ca, (denoted by a_{Ca}), measured at constant concentration of Ficoll 70 at approximately even increments of the logarithm of a_{Ca}, in the absence of Ficoll and at four different concentrations of Ficoll.

It is assumed that in the absence of Ca, RCL exists entirely in the A state, and that the fractional change in FIR upon addition of Ca is equal to the fraction of H state (f_H), since the tryptophan reporter residues are not within any of the Ca-binding motifs (SP Fig. S1, see ref. 2).

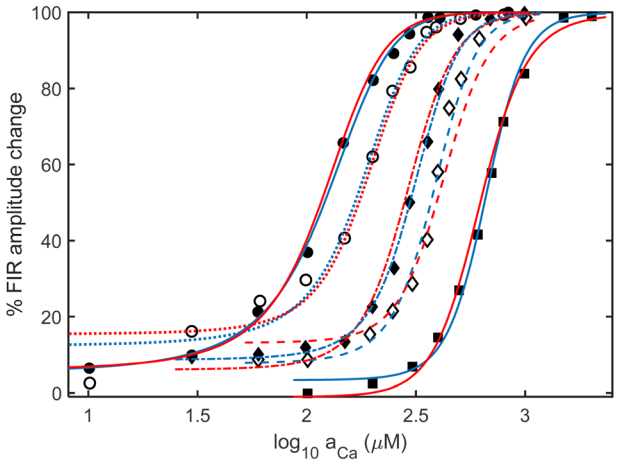

Fig. 2 Fractional change in fluorescence intensity ratio (FIR) *vs.* logarithm of the thermodynamic activity of Ca (a_{Ca}) at 25 °C, in the presence of the following concentrations of Ficoll 70: 0 (squares), 0.1 g cm^{-3} (open diamonds), 0.2 g cm^{-3} (closed diamonds), 0.3 g cm^{-3} (open circles), 0.4 g cm^{-3} (closed circles). Blue and red curves are calculated using best fit values of model functions obtained as described in the text.

Given values of the model parameters n, K_A, z, and L defined in the previous section, one may then use eqn (14) to calculate the fraction of RCL in the H conformation. The first three of these parameters are assumed to be independent of Ficoll concentration, while the logarithm of L is predicted to vary linearly with Ficoll concentration according to eqn (18). The conversion from f_H to FIR requires additional specification of the values of the four empirical parameters s_{11}, s_{12}, s_{21}, and s_{22} defined in eqn (S1) and (S2) (ESI†). Examination of the data plotted in Fig. 2A of SP suggests that the values of s_{12} and s_{22} may be fixed equal to 0, and the value of s_{21} may be fixed equal to 100. However, the asymptotic limit of FIR in the limit of low Ca concentration appears to vary between data sets, and so we allow one additional parameter, s_{11}, to vary to achieve a best fit of the model to each data set. Thus, global modeling of the data for the five data sets obtained at different Ficoll concentrations requires specification of the values of the three global parameters n, K_A, and z, plus one value of L and one value of s_{11} for each Ficoll concentration, or 13 parameters in all.

Initially, the data plotted in Fig. 2 were modeled using eqn (8) and eqn (S1) and (S2) (ESI†) to calculate the best fit of the model to the measured dependence of FIR upon a_{Ca}. This was accomplished by allowing the values of each of the parameters listed in column 1 of Table S1 (ESI†) to vary in order to achieve simultaneous minimization of the sum-of-squared residuals for all five data sets (w_{Fic} = 0, 0.1, 0.2, 0.3, and 0.4 g mL^{-1}) plotted in Fig. 2. We refer to this as the independent L model. The best-fit dependence of FIR upon a_{Ca} to all five data sets calculated according to the independent L model is plotted as blue curves in Fig. 2. The best fit values of the input parameters are presented in column 2 of Table S1 (ESI†), and the best-fit values of ln L are plotted as a function of Ficoll concentration in

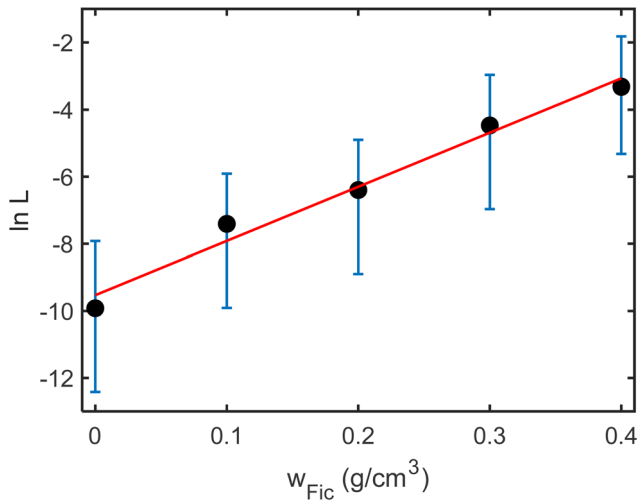

Fig. 3 Best fit values of ln L obtained by global least-squares fitting of the data by the independent L model, plotted as a function of w_{Fic}. Error bars correspond to one standard error of estimate calculated *via* parameter scanning.[28] Also plotted is the best-fit straight line through the points, with a slope of 16.1 cm^3 g^{-1} Ficoll.

Fig. 3. It may be seen that the results are well described by the linear dependence predicted by the excluded volume model relation (18), with $\alpha_{AH} \cong 16.1$ cm^3 g^{-1}.

Given the success of modeling with independently variable values of ln L, the data were subsequently modeled using the same equations, except that the values of ln L at different Ficoll concentrations were constrained to obey the linear dependence indicated in eqn (18), and only ln L_0 and α_{AH} are allowed to vary instead of the five independent values of ln L. We refer to this approach as the constrained L model, which requires only 10 variable parameters rather than 13. The best-fit dependence of FIR upon a_{Ca} to all five data sets calculated using the constrained L model is plotted as red curves in Fig. 2, and the best fit values of the input parameters are presented in column 3 of Table S1 (ESI†). The best-fit value of α_{AH} obtained with the constrained L model is approximately 15.4 cm^3 g^{-1}, which agrees with the value of 16.1 obtained indirectly *via* the unconstrained model to within 5%. We conclude that the effect of Ficoll on the calcium-induced two-state conformational change at 25 °C is satisfactorily described by the constrained L model, according to the first order excluded volume treatment summarized in text eqn (5) and (18).

IV. Dependence of RCL conformation upon temperature and Ficoll concentration in the absence and presence of calcium

A. Description of the excluded volume model

It is assumed that an increase in temperature leads to conversion of a more folded conformational state 1 (representing either H or A) to a less folded state 2 (representing either H* or A*). It is further assumed that the addition of an "inert" crowding species C does not affect the properties of either conformational state. Justification for these assumptions is provided in the Discussion. The calculation of the temperature dependence of f_2 follows that utilized by SP, summarized below and generalized to allow for the effect of volume excluded by C to the trace protein undergoing unfolding.

The fraction of protein that is unfolded as a function of temperature is given by

$$f_2(T) = \frac{K_{12}(T)}{1 + K_{12}(T)} \tag{19}$$

where $K_{12}(T)$ is the apparent equilibrium constant relating the concentrations of states 1 and 2:

$$K_{12}(T) = c_2/c_1 = \exp(-\Delta G_{12}(T)/RT). \tag{20}$$

Here ΔG_{12} denotes the temperature-dependent change in Gibbs free energy accompanying the transition between states 1 and 2, given by the Gibbs–Helmholtz relation[20]

$$\Delta G_{12}(T) = \Delta H_{T_m}(1 - T/T_m) - \Delta C_P[T_m - T + T\ln(T/T_m)] \tag{21}$$

where R denotes the molar gas constant, T the absolute temperature, T_m denotes the temperature at which the protein is half-unfolded, ΔH_{T_m} the enthalpy change of unfolding at T_m, and ΔC_p the heat capacity change, assumed to be independent of temperature and the concentration of crowder.

It is assumed that the Ficoll concentration dependence of K_{12} and the thermal unfolding curve *via* eqn (19) is calculated according to the first-order excluded volume model eqn (5).

B. Modeling the data

The two-state model presented above provides relations for the calculation of the value of the fraction of thermally unfolded conformation (H* in the presence of Ca and A* in the absence of Ca) as a function of temperature and Ficoll concentration.

It is assumed that in the low temperature limit, RCL exists entirely in the apo (A) state in the absence of Ca and entirely in the holo (H) state in the limit of saturating concentration of Ca. It is further assumed that in the high temperature limit, RCL exists entirely in the A* state in the absence of Ca and entirely in the H* state in the presence of high Ca concentration.

Given the values of T_m, ΔH_{T_m} and ΔC_p, eqn (20) and (21) are used to calculate the value of $K^0_{AA^*}$ (in the absence of Ca and Ficoll) and $K^0_{HH^*}$ (in the presence of high Ca and the absence of Ficoll) as a function of temperature. Then eqn (5) and (19) together with specified values of α_{AA^*} and α_{HH^*} are then used to calculate the dependence of f_{A^*} and f_{H^*} upon temperature and Ficoll concentration. Finally, eqn (S1) and (S2) (ESI†) are used to calculate the dependence of the experimentally measured signal upon both temperature and Ficoll concentration. Non-linear least-squares modeling was used to globally fit the two-state excluded volume model for thermal unfolding of holo to the temperature dependence of ellipticity of RCL measured in the presence of 5 mM Ca and in the absence and presence of Ficoll 70 plotted in Fig. 4A. The curves calculated using the best-fit parameter values presented in column 1 of Table S2 (ESI†) are plotted together with the data. Using the same model

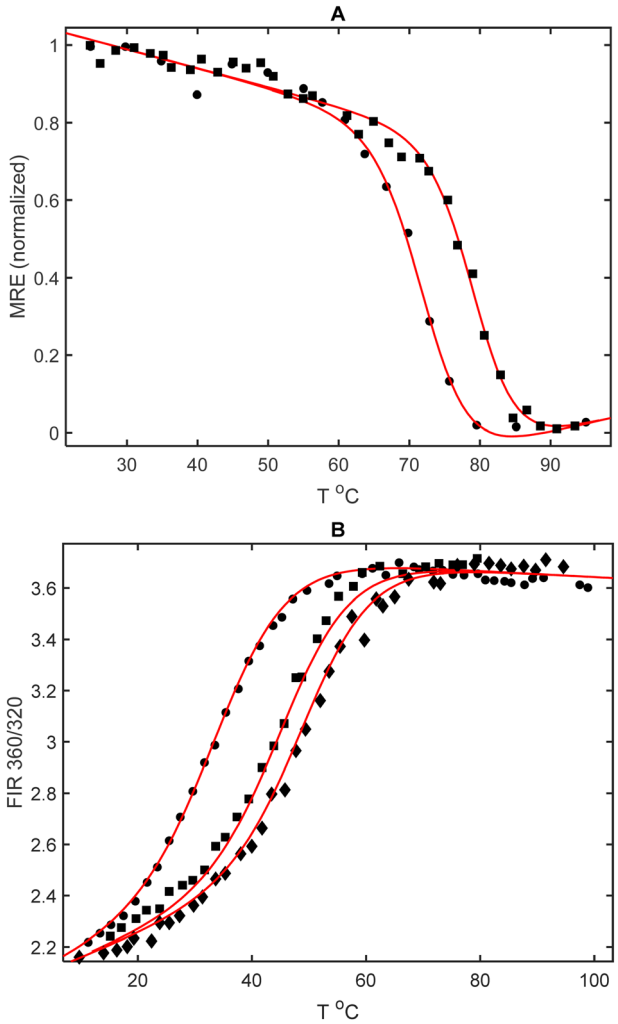

Fig. 4 Data and best-fit model calculation of the dependence of experimentally measured signal of conformational change of RCL as a function of temperature. (A) normalized mean residual ellipticity (MRE) of RCL in the presence of 5 mM Ca (H → H*). MRE (normalized) ≡ (MRE − MRE_{min})/(MRE_{max} − MRE_{min}). Ficoll: 0 (circles), 200 g l^{-1} (squares). (B) FIR of RCL in the absence of Ca (A → A*). Ficoll: 0 (circles), 0.3 g cm^{-3} (squares), 0.4 g cm^{-3} (diamonds). Best fit model parameter values are reported in Table S2 (ESI†).

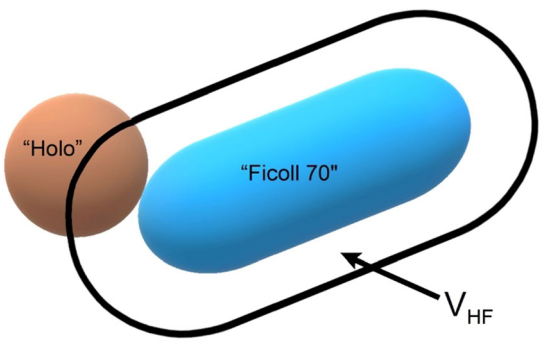

Fig. 5 Equivalent hard particle representation of holo as a sphere and Ficoll 70 as a spherocylinder (not to scale). The covolume of the two particles is the volume excluded to the center of the sphere by the spherocylinder, the surface of which is indicated by the black line.

equations, the two-state excluded volume model for the thermal unfolding of apo was then globally fit to the temperature dependence of the fluorescence intensity ratio of RCL measured in the absence of Ca and in the absence and presence of Ficoll 70, plotted in Fig. 4B. The curves calculated using the best-fit parameter values presented in column 2 of Table S2 (ESI†) are plotted together with the data. We conclude that the experimental data measuring the effect of Ficoll 70 on the temperature-dependent conformational change of RCL in the presence of high Ca (H → H*) and the absence of Ca (A → A*) are well accounted for by the two-state excluded volume model presented here.

V. Characterization of the interaction between Ficoll 70 and the four conformational states of RCL

In the preceding two sections, two-state models have been successfully fit to the data obtained from measurements by SP of the effect of high concentrations of Ficoll 70 upon (i) a calcium-induced conformational change at low temperature and (ii) thermally-induced unfolding in the absence and presence of calcium. These have led to approximate evaluations of the following three parameters:

$$\begin{aligned} \alpha_{AH} &= V_{AF} - V_{HF} \sim 15\,\mathrm{cm^3\,g^{-1}} \\ \alpha_{HH^*} &= V_{HF} - V_{H^*F} \sim -11\,\mathrm{cm^3\,g^{-1}} \\ \alpha_{AA^*} &= V_{AF} - V_{A^*F} \sim -6\,\mathrm{cm^3\,g^{-1}} \end{aligned} \tag{22}$$

where V_{XF} denotes the volume excluded by a molecule of X to a molecule of Ficoll in units of inverse concentration. Combination of these values leads to

$$\begin{aligned} V_{H^*F} &\sim V_{HF} + 11\,\mathrm{cm^3\,g^{-1}} \\ V_{A^*F} &\sim V_{HF} + 21\,\mathrm{cm^3\,g^{-1}} \\ V_{A^*F} &\sim V_{H^*F} + 10\,\mathrm{cm^3\,g^{-1}} \end{aligned} \tag{23}$$

The covolume of holo-RCL and Ficoll 70 cannot be evaluated from the data of SP, but a rough estimate of its value may be made given the results of earlier nonideal tracer sedimentation equilibrium measurements,[29] which were interpreted in the context of a model in which proteins and other macromolecules are represented as equivalent hard convex particles. The equivalent hard convex particle representation of Ficoll 70 best accounting for the thermodynamic interaction of Ficoll and BSA, depicted schematically in Fig. 5, was found to be a spherocylinder with a cylindrical radius of ∼1.4 nm and a cylindrical length of ∼15.7 nm.[29] The equivalent hard convex particle representation of holo-RCL, the most compact of the conformations in the four-state model, is assumed to be approximately spherical. Given the molar mass (17 100 g mol^{-1})[7] and density (0.72 $cm^3\ g^{-1}$)[30] of RCL, the radius of the equivalent spherical particle representing holo-RCL, depicted schematically in Fig. 5, is calculated to be ∼1.7 nm.[15] The

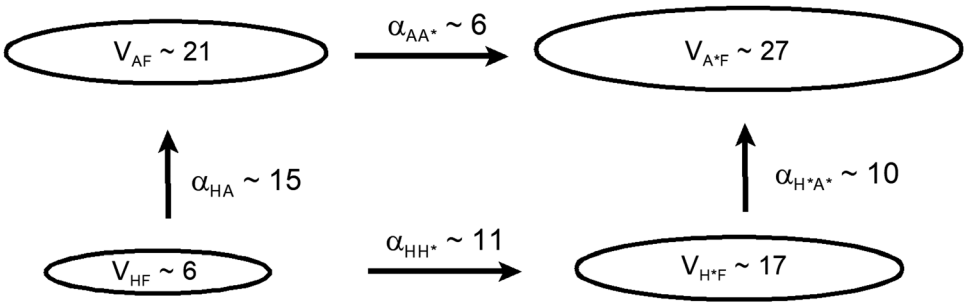

Fig. 6 Estimated covolumes of each of the four conformational states of RCL with Ficoll 70, calculated as described in the text. These results indicate that the relative extension (*i.e.*, Ficoll exclusion volume) of each state increases in the order H < H* < A < A*.

covolume of these two hard convex particles, calculated using relations presented in ref. 26, is ~6 cm^3 g^{-1}. Assuming that this estimate is semi-quantitatively valid, the numeric relations presented above lead to estimates of the covolumes of each of the four conformational states of RCL, in units of cm^3 g^{-1}-Ficoll, shown in Fig. 6.

VI. Conclusions

The analysis presented here is based upon application of the effective hard particle model for interpretation of intermolecular interactions. We recognize that this model represents a simplified parameterization of interaction coefficients, and that the calculation of covolumes of equivalent hard particles representing partially or fully unfolded proteins or polymers is subject to some uncertainty.[31] Nonetheless, the effective hard particle model has proven to provide a self-consistent and semi-quantitative interpretation of a variety of measurements of the concentration-dependent behavior of proteins and protein mixtures in highly nonideal solutions.

Analysis of the combined measurements of the effect of Ficoll on both the chemically induced folding of A to H at constant temperature and the thermally induced unfolding of both A and H to A* and H*, respectively, within the context of the effective hard particle model permits a simple yet comprehensive and quantitative interpretation of a large number of experimental results, summarized in Fig. 2 and 4. This analysis leads to the following qualitative conclusions about the relative net interaction of Ficoll 70 with each of the four conformational states of RCL identified by SP.

(1) The transition between H and A is accompanied by a significantly greater change in repulsive interaction with Ficoll 70 than the transition between H and H*.

(2) The transition between A and A* is accompanied by a significantly smaller change in repulsive interaction with Ficoll 70 than the transition between H and H*.

In the previous section, the difference between V_{A^*F} and V_{AF} was estimated to be ~6 cm^3 g^{-1}, and the difference between V_{HF} and V_{H^*F} to be ~11 cm^3 g^{-1}. Assuming that the differences between these several covolumes is due primarily to the difference between the Ficoll exclusion volumes of the effective spherical (or quasi-spherical) particles representing the various conformational states of RCL, this result suggests that the thermal unfolding of A in the absence of Ficoll is associated with a significantly smaller "expansion" of RCL than the thermal unfolding of H in the absence of Ficoll. If we additionally assume that "expansion" is correlated with a loss of attractive intramolecular interactions, then the two conclusions enumerated above are in qualitative accord with the observation that in the absence of Ficoll, thermally-induced unfolding of A is accompanied by a significantly smaller change in enthalpy and free energy than the thermally-induced unfolding of H (SP and Table S2 of ESI†).

The compacting effect of addition of Ca upon RCL folding is due to a combination of two factors. First, binding of Ca to ~8–9 specific sites on RCL leads to acquisition of localized secondary and tertiary structure, presumably resulting in some measure of overall compaction. Second, the addition of Ca at concentrations encountered in the experiments of SP (up to 5 mM) results in a substantial increase in the ionic strength of the solution, which acts nonspecifically to damp out the predominantly repulsive electrostatic interactions driving conformational expansion.[32] The nonspecific effect of increasing ionic strength upon protein compaction has been experimentally observed upon addition of NaCl to solutions of RD,[13] a protein with calcium-binding properties similar to those of RCL.[14,16] Thermally induced unfolding, on the other hand, is due primarily to the nonspecific enhancement at high temperature of entropic contributions to the free energy of conformational change. According to the model of the energetics of conformational change associated with calcium binding described in Section II.1, apo retains the ability to bind calcium to specific sites, although with an affinity that is approximately 10-fold smaller than that of holo (Table S1, ESI†). In the presence of very high concentrations of Ca (on the order of 5 mM) entropic effects alone would probably be insufficient at high temperature to result in complete dissociation of Ca from RCL, so H* would likely retain some residual Ca-linked stabilization relative to H.

In bacterial cytoplasm at a host temperature of 37 °C, in the absence of calcium and in the presence of a collectively high concentration of biomolecules, RCL exists as an equilibrium mixture of the intrinsically disordered A state and the fully thermally unfolded A* conformations, as shown in Fig. 4B. The model described in text Section IV may be used together with the values of the best-fit parameters presented in column 3 of

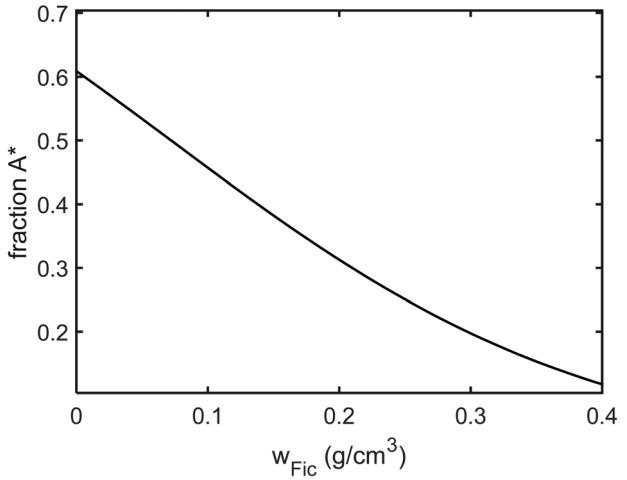

Fig. 7 Ficoll dependence of the fraction of apo existing as A* in an equilibrium mixture of A + A* at 37°, calculated using the excluded volume model described in the text.

Table S2 (ESI†) to calculate the equilibrium fraction of apo existing in the fully unfolded state A* at 37 °C as a function of Ficoll concentration, and the results are plotted in Fig. 7. It may be seen that the addition of Ficoll to a concentration comparable to the total concentration of macromolecules in the cytoplasm of *E. coli* reported by Zimmerman and Trach[33] (0.3–0.4 g cm^{-3}) reduces the equilibrium fraction of A* at 37° from ~0.6 to less than 0.2. While this calculation is much too simple to accurately portray the effect of volume exclusion within bacterial cytoplasm, it is nevertheless of qualitative value as indicating how crowding-induced partial compaction of apo-RCL (from A* to A state) could influence its interaction with the specific secretion channel T1SS and the consequent kinetics of secretion. The molecular basis of this interaction and its ramifications for regulation of toxin secretion is the subject of current research.

Data availability

There are no original experimental data in this manuscript. The manuscript states that the MATLAB code used to model data taken from the publication of Sotomayor-Perez *et al.* (ref. 2 of the MS) is available upon request.

Conflicts of interest

There are no conflicts to declare.

Acknowledgements

Research of AC is supported by Institut Pasteur (SPAIS and DARRI grants), CNRS (Centre National de la Recherche Scientifique) and ANR (Agence Nationale pour la Recherche). Research of APM is supported by the Intramural Research Program of the National Institute of Diabetes and Digestive and Kidney Diseases. The authors thank Dr Peter McPhie (NIH) for helpful comments on an early draft of this report. APM dedicates his contribution to Prof. Judith Herzberg, in honor of her contributions to the understanding of excluded volume effects in crowded multicomponent fluids.

References

1 A. C. Sotomayor-Perez, D. Ladant and A. Chenal, Disorder-to-order transition in the CyaA toxin RTX domain: implications for toxin secretion, *Toxins Basel*, 2015, **7**, 1–20.
2 A. C. Sotomayor-Perez, O. Subrini, A. Hessel, D. Ladant and A. Chenal, Molecular Crowding Stabilizes Both the Intrinsically Disordered Calcium-Free State and the Folded Calcium-Bound State of a Repeat in Toxin (RTX) Protein, *J. Am. Chem. Soc.*, 2013, **135**, 11929–11934.
3 N. Guiso, Bordetella Adenylate Cyclase-Hemolysin Toxins, *Toxins*, 2017, **9**, 277.
4 J. Novak, O. Cerny, A. Osickova, I. Linhartova, J. Masin, L. Bumba, P. Sebo and R. Osicka, Structure-Function Relationships Underlying the Capacity of Bordetella Adenylate Cyclase Toxin to Disarm Host Phagocytes, *Toxins*, 2017, **9**, 300.
5 D. P. O'Brien, A. C. S. Perez, J. Karst, S. E. Cannella, V. Y. N. Enguéné, A. Hessel, D. Raoux-Barbot, A. Voegele, O. Subrini, M. Davi, J. I. Guijarro, B. Raynal, B. Baron, P. England, B. Hernandez, M. Ghomi, V. Hourdel, C. Malosse, J. Chamot-Rooke, P. Vachette, D. Durand, S. Brier, D. Ladant and A. Chenal, Calcium-dependent disorder-to-order transitions are central to the secretion and folding of the CyaA toxin of Bordetella pertussis, the causative agent of whooping cough, *Toxicon Off. J. Int. Soc. Toxinol.*, 2018, **149**, 37–44.
6 A. Voegele, D. P. O'Brien, O. Subrini, N. Sapay, S. E. Cannella, V. Y. N. Enguene, A. Hessel, J. Karst, V. Hourdel, A. C. S. Perez, M. Davi, R. Veneziano, J. Chopineau, P. Vachette, D. Durand, S. Brier, D. Ladant and A. Chenal, Translocation and calmodulin-activation of the adenylate cyclase toxin (CyaA) of Bordetella pertussis, *Pathog. Dis.*, 2018, **76**, fty085.
7 A. C. Sotomayor Perez, J. C. Karst, M. Davi, J. I. Guijarro, D. Ladant and A. Chenal, Characterization of the regions involved in the calcium-induced folding of the intrinsically disordered RTX motifs from the bordetella pertussis adenylate cyclase toxin, *J. Mol. Biol.*, 2010, **397**, 534–549.
8 C. Bauche, A. Chenal, O. Knapp, C. Bodenreider, R. Benz, A. Chaffotte and D. Ladant, Structural and functional characterization of an essential RTX subdomain of Bordetella pertussis adenylate cyclase toxin, *J. Biol. Chem.*, 2006, **281**, 16914–16926.
9 J. C. Karst, V. Y. Ntsogo Enguene, S. E. Cannella, O. Subrini, A. Hessel, S. Debard, D. Ladant and A. Chenal, Calcium, Acylation, and Molecular Confinement Favor Folding of Bordetella pertussis Adenylate Cyclase CyaA Toxin into a Monomeric and Cytotoxic Form, *J. Biol. Chem.*, 2014, **289**, 30702–30716.

10 S. E. Cannella, V. Y. Ntsogo Enguene, M. Davi, C. Malosse, A. C. Sotomayor Perez, J. Chamot-Rooke, P. Vachette, D. Durand, D. Ladant and A. Chenal, Stability, structural and functional properties of a monomeric, calcium-loaded adenylate cyclase toxin, CyaA, from Bordetella pertussis, *Sci. Rep.*, 2017, **7**, 42065.
11 D. P. O'Brien, S. E. Cannella, A. Voegele, D. Raoux-Barbot, M. Davi, T. Douche, M. Matondo, S. Brier, D. Ladant and A. Chenal, Post-translational acylation controls the folding and functions of the CyaA RTX toxin, *FASEB J.*, 2019, **33**, fj201802442RR.
12 A. Voegele, M. Sadi, D. P. O'Brien, P. Gehan, D. Raoux-Barbot, M. Davi, S. Hoos, S. Brûlé, B. Raynal, P. Weber, A. Mechaly, A. Haouz, N. Rodriguez, P. Vachette, D. Durand, S. Brier, D. Ladant and A. Chenal, A High-Affinity Calmodulin-Binding Site in the CyaA Toxin Translocation Domain is Essential for Invasion of Eukaryotic Cells, *Adv. Sci.*, 2021, **8**, 2003630.
13 A. Chenal, J. C. Karst, A. C. Sotomayor Perez, A. K. Wozniak, B. Baron, P. England and D. Ladant, Calcium-induced folding and stabilization of the intrinsically disordered RTX domain of the CyaA toxin, *Biophys. J.*, 2010, **99**, 3744–3753.
14 A. Chenal, J. I. Guijarro, B. Raynal, M. Delepierre and D. Ladant, RTX calcium binding motifs are intrinsically disordered in the absence of calcium: implication for protein secretion, *J. Biol. Chem.*, 2009, **284**, 1781–1789.
15 A. C. Sotomayor-Perez, D. Ladant and A. Chenal, Calcium-induced folding of intrinsically disordered repeat-in-toxin (RTX) motifs via changes of protein charges and oligomerization states, *J. Biol. Chem.*, 2011, **286**, 16997–17004.
16 D. P. O'Brien, B. Hernandez, D. Durand, V. Hourdel, A. C. Sotomayor-Perez, P. Vachette, M. Ghomi, J. Chamot-Rooke, D. Ladant, S. Brier and A. Chenal, Structural models of intrinsically disordered and calcium-bound folded states of a protein adapted for secretion, *Sci. Rep.*, 2015, **5**, 14223.
17 L. Bumba, J. Masin, P. Macek, T. Wald, L. Motlova, I. Bibova, N. Klimova, L. Bednarova, V. Veverka, M. Kachala, D. I. Svergun, C. Barinka and P. Sebo, Calcium-Driven Folding of RTX Domain beta-Rolls Ratchets Translocation of RTX Proteins through Type I Secretion Ducts, *Mol. Cell*, 2016, **62**, 47–62.
18 A. Chenal, A. C. Sotomayor Perez and D. Ladant, *The Comprehensive Sourcebook of Bacterial Protein Toxins*, Elsevier, 4th edn, 2015.
19 S. L. Speer, C. J. Stewart and L. Sapir, Macromolecular Crowding is More Than Hard-Core Repulsions, *Annu. Rev. Biophys.*, 2022, **51**, 267–300.
20 W. J. Becktel and J. A. Schellman, Protein Stability Curves, *Biopolymers*, 1987, **26**, 1859–1877.
21 G. Rivas and A. P. Minton, Toward an understanding of biochemical equilibria in living cells, *Biophys. Rev.*, 2018, **10**, 241–253.
22 W. G. McMillan Jr and J. E. Mayer, The statistical thermodynamics of multicomponent systems, *J. Chem. Phys.*, 1945, **13**, 276–305.
23 A. P. Minton and H. Edelhoch, Light scattering of bovine serum albumin solutions: extension of the hard particle model to allow for electrostatic repulsion, *Biopolymers*, 1982, **21**, 451–458.
24 A. P. Minton, A molecular model for the dependence of the osmotic pressure of bovine serum albumin upon concentration and pH, *Biophys. Chem.*, 1995, **57**, 65–70.
25 A. P. Minton, The effective hard particle model provides a simple, robust, and broadly applicable description of non-ideal behavior in concentrated solutions of bovine serum albumin and other nonassociating proteins, *J. Pharm. Sci.*, 2007, **96**, 3466–3469.
26 A. P. Minton, Molecular Crowding: Analysis of Effects of High Concentrations of Inert Cosolutes on Biochemical Equilibria and Rates in Terms of Volume Exclusion, *Methods Enzymol.*, 1998, **295**, 127–149.
27 J. Monod, J. Wyman and J. P. Changeux, On the nature of allosteric interactions: a plausible model, *J. Mol. Biol.*, 1965, **12**, 88–118.
28 H. A. Saroff, Evaluation of uncertainties for parameters in binding studies: the sum-of-squares profile and Monte Carlo estimation, *Anal. Biochem.*, 1989, **176**, 161–169.
29 A. A. Fodeke and A. P. Minton, Quantitative Characterization of Polymer-Polymer, Protein-Protein, and Polymer-Protein Interaction via Tracer Sedimentation Equilibrium, *J. Phys. Chem. B*, 2010, **114**, 10876–10880.
30 A. K. Attri and A. P. Minton, An Automated Method for Determination of the Molecular Weight of Macromolecules via Sedimentation Equilibrium in a Preparative Ultracentrifuge, *Anal. Biochem.*, 1983, **133**, 142–152.
31 A. P. Minton, Models for excluded volume interaction between an unfolded protein and rigid macromolecular cosolutes: macromolecular crowding and protein stability revisited, *Biophys. J.*, 2005, **88**, 971–985.
32 C. Tanford, *Physical Chemistry of Macromolecules*, Wiley & Sons, New York, 1961.
33 S. B. Zimmerman and S. O. Trach, Estimation of macromolecule concentrations and excluded volume effects for the cytoplasm of Escherichia coli, *J. Mol. Biol.*, 1991, **222**, 599–620.